Structural, magnetic and optical properties of Cr doped $CeFeO_3$ nanoparticles synthesized by co-precipitation method

K.selvam[1], S.**Jeeva**[2] and **G.Mani**[*]

[1,2,*]Dept of Physics, Arignar Anna Govt. Arts College, Cheyyar, Tamil Nadu, India -604407.

ABSTRACT

Structure, Characterization and magnetic properties of Cr-doped $CeFeO_3$ ($CeFe_{1-x}Cr_xO_3$) nanoparticles have been synthesized by co-precipitation method. The consequential samples are characterized by structural, optical and magnetic properties. The average crystallite size (D_c) is decreasing with a dopant and establish to be altering between 7nm-32.6nm. The morphology is analyzed using scanning electron microscope and the obtained results credited that E_g values are growing with dopant varying between 2.05 eV- 2.61 eV.The metal oxide (M-O) stretching vibrations and few functional groups are detected from infrared spectra. (VSM) Vibrating sample magnetometer analysed the weak ferromagnetic behavior is pragmatic from hysteresis loop behavior. As well, the large hysteresis loop behavior induces no saturation up to 15kOe in nanoparticles. According to the obtained grades, $CeFeO_3$ nanopowder can be raised as a visible light-driven photocatalyst,

Keywords: Crystallite size, Co-precipitation method, Nanoparticles, optical properties, Magnetic Properties.

1. INTRODUCTION

In recent years, perovskite oxides with common formula ABO_3 have ensnared much thought because of the properties that effect from highly correlated d-band strong electron–lattice couplings and electrons. In addition, are very essential materials exhibiting special properties such as ferroelectricity [1,2,3], huge magnetoresistance and ferromagnetism [4,5],dielectric properties, piezoelectricity, [6,7], and semiconductivity [8].

The Fe-O-Fe bond angle is a scale to analyse the degree of deformation which affects the structural, optical, dielectric, magnetic and other properties of the compound [9]. Nowadays, $RFeO_3$ceramic objects have been the target of thought of researchers due to their helpful properties in different applications ranging from solid oxide fuel cells [10], sensors [11], environmental catalysts [12] to magnetic materials [13]. As

well, high domain-wall velocity as well as the continuation of Bloch lines production them applicable in magneto-optical data storage devices [14].

Mixed oxides type photocatalysts as well as perovskite (ABO_3) type structures are also between the large number of photocatalyst compositions explored [15]. TiO_2[16, 17], $SrTiO_3$ [18] and $NaTaO_3$[19] are between the most possible photocatalysts for hydrogen generation because they have benign stability, immobile nature and thermodynamically optimum band structures. The co -precipitation is the main method for the research of $CeFeO_3$[20–21], in which the precursors of $CeFeO_3$ are first prepared and then subjected to high temperature calcinations. The $CeFeO_3$ is a narrow band gap semiconductor material, which has large view for applications in visible-light photocatalysis [22-23].

2. EXPERIMENTAL TECHNIQUES

$CeFe_{1-x}Cr_xO_3$ ceramic powders are synthesized by Co-precipitation method with the aqueous solutions of Ce $(NO_3)_2.6H_2O$ (99.6 % purity, Sigma-Aldrich), Fe $(NO_3)_2.9H_2O$ (99.6 % purity, Sigma-Aldrich) and $Cr(NO_3)_2.6H_2O$ (99.6 % purity, Sigma-Aldrich) mixtures respectively in alkaline medium. The solutions of Ce $(NO_3)_26H_2O$, Fe $(NO_3)_2.9H_2O$ and $Cr(NO_3)_2.6H_2O$in their stoichiometry (1g of $Ce(NO_3)_2.6H_2O$ in 50 ml), (0.8g of Fe $(NO_3)_2.9H_2O$ in 50 ml), (0.2g of $Cr(NO_3)_2.6H_2O$ in 50 ml) were dissolved in double distilled water with a constant stirring. The pH maintained in between 10-11 by adding NaOH solution was additional drop wise to the mixture. Later, the solution forms a precipitate which was stirred (350 rotation/min) at room temperature for 30 min and then kept at 80°C for 3 hrs. The resultant sample was chilled to room temperature. The sample is filtered and washed several times with double distilled water. The sample was then dried at 100°C for over night. The dried sample was downy mass in form that is grind for 2hrs, and the consequential powder was sintered for 3hrs at 800°C. After sintering the sample is once more grinded for 4hrs using the Motor pestle apparatus and the resulting powder is analysed to XRD, FTIR, SEM / EDAX and VSM.

3. RESULTS AND DISSCUSSION

3.1 XRD analysis

XRD pattern depicts the $CeFe_{1-x}Cr_xO_3$ nanoparticles as shown in figure(1). All the reflection planes are in good agreement with the standard JCPDS: 22-0166 of orthorhombic structure. The maximum intensity peak was observed at 32.3^0corresponding to (112) plane of $CeFeO_3$ structure. Other characteristics peaks at 2θ values 22.6^0, 39.8^0,46.5^0, 52.5^0, 57.8^0, $67.6^0$and 77^0 were besides observed for respective planes of (002), (202), (004), (311), (204), (224) and (116). All the peaks obtained in XRD pattern are intense and sharp, which suggests highly crystalline orthorhombic single phase of nanoparticle $CeFeO_3$ material, synthesized by Co-precipitation method. The average diameter (D) of the sample is evaluated for the intense peak positions using Scherrer's formula [24]:

$$D = \frac{k\lambda}{\beta \cos\theta} \text{--------(1)}$$

Where 'k' is a constant and is approximately equals to 0.9 for a spherical symmetry, 'λ' is X-ray wavelength of CuK_α = 1.5418 Å, 'θ' is diffraction angle and 'β' is full-width half maxima (FWHM).

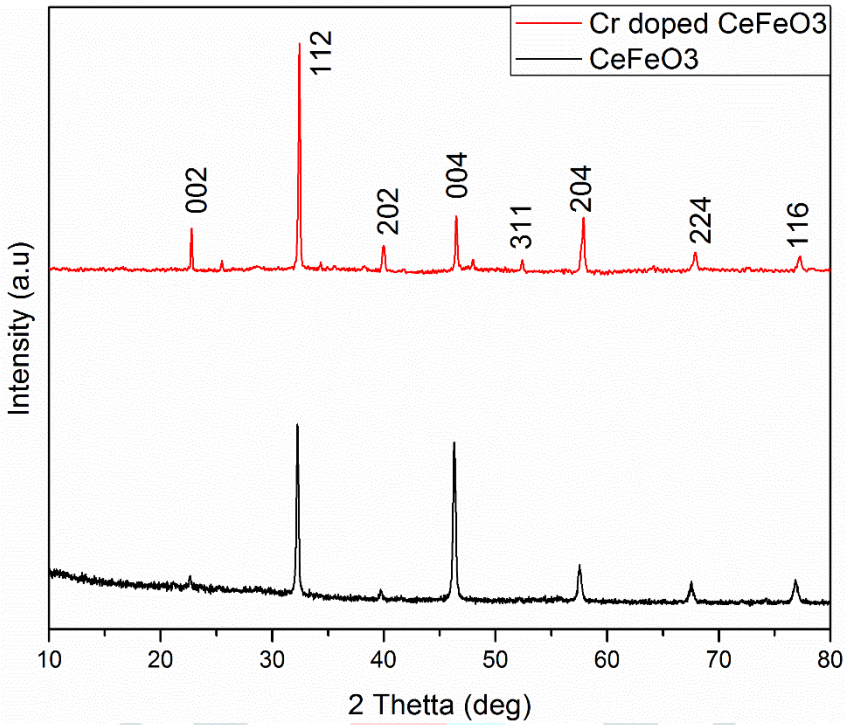

Figure 1: XRD pattern of $CeFeO_3$ and $CeFe_{1-x}Cr_xO_3$ (x =0, 0.2)

3.2 FTIR ANALYSIS

The Fourier transform infrared spectra (FT-IR) of $CeFe_{1-x}Cr_xo_3$ (x=0, 0.2) nanopowders. The absorption bands are formed. The higher wave number metal oxide (M-O) 848.66 cm^{-1} – 877.61 cm^{-1} this range is approximately 3462.22 cm^{-1} are more absorption bands observed (25). Which are assigned to the asymmetry stretching mode and symmetry of water molecules. At approximately 1435.04 cm^{-1} and 1639.4 cm^{-1} wave number the bending mode is O-H band are observed. The peak is 848.66 cm^{-1} reveals in very small absorption presence of metal oxide bonds. The vibration modes Fe – O and O –Fe –O bands (26).

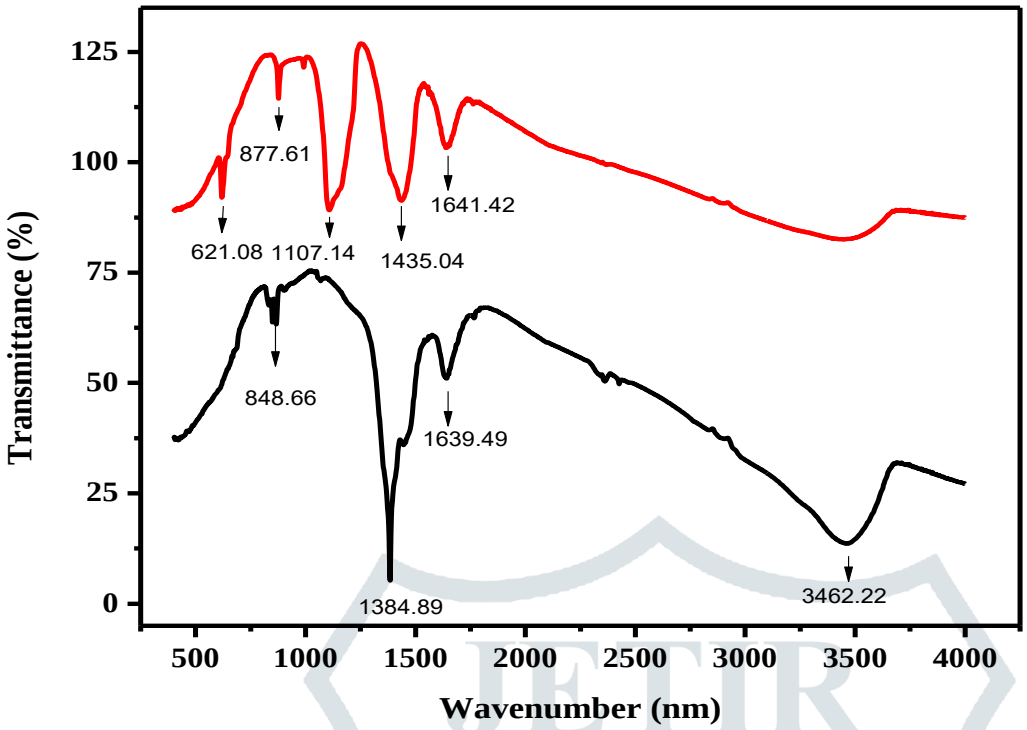

Fig.(2) FTIR spectra of $CeFe_{1-x}Cr_xO_3$ (x = 0, 0.2)

3.3 Surface Morphology

Surface morphology and Elemental analysis of nanoparticles are characterized by (SEM) scanning electron microscope and Energy dispersive X-ray (EDX). As much as the shape is concerned x = 0 & 0.2 showed the flat plate-like grains. Figure 3 (a) shows the SEM photographs, the particle size around 28.11-28.67 nm grains were found. SEM images of the local morphological of $CeFeO_3$ and $CeCr_xFe_{1-x}0_3$ images show good nanocrystalline grains.

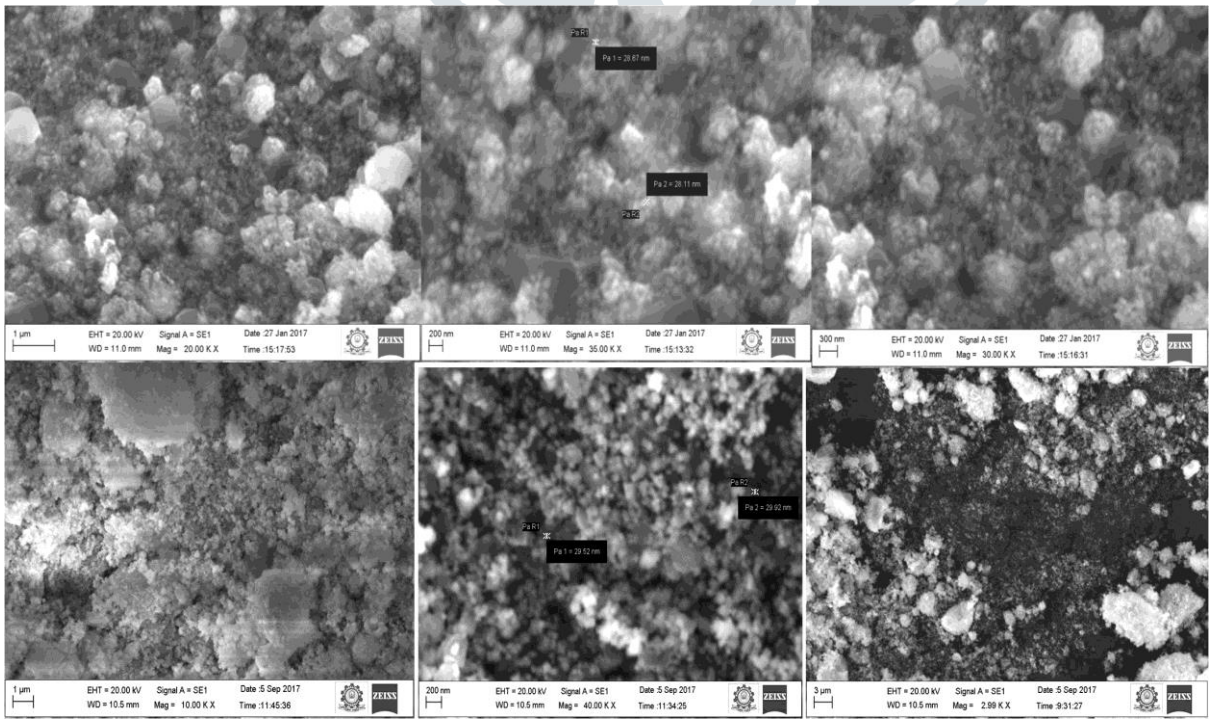

Fig.3 (a) SEM photographs of $CeFeO_3$ and $CeFe_{1-x}Cr_xO_3$(x=0, 0.2)

The EDX results confirm the elemental pattern of samples as illustration in Figure 3(b). The peaks of Ce, Fe, Cr and O were professed for all samples. We also apparent peaks of Cr for the samples with x = 0.2. It is found that the enhanced elements of Cr atomic replies to the reduction of that of Fe atomic as well as the increase of Cr content. It designates that the substitution of Cr ions into Fe site is complete. The presence of Cr, Fe, Ce and O elements including their atomic (At%) and weight (Wt%) percentzages are reported.

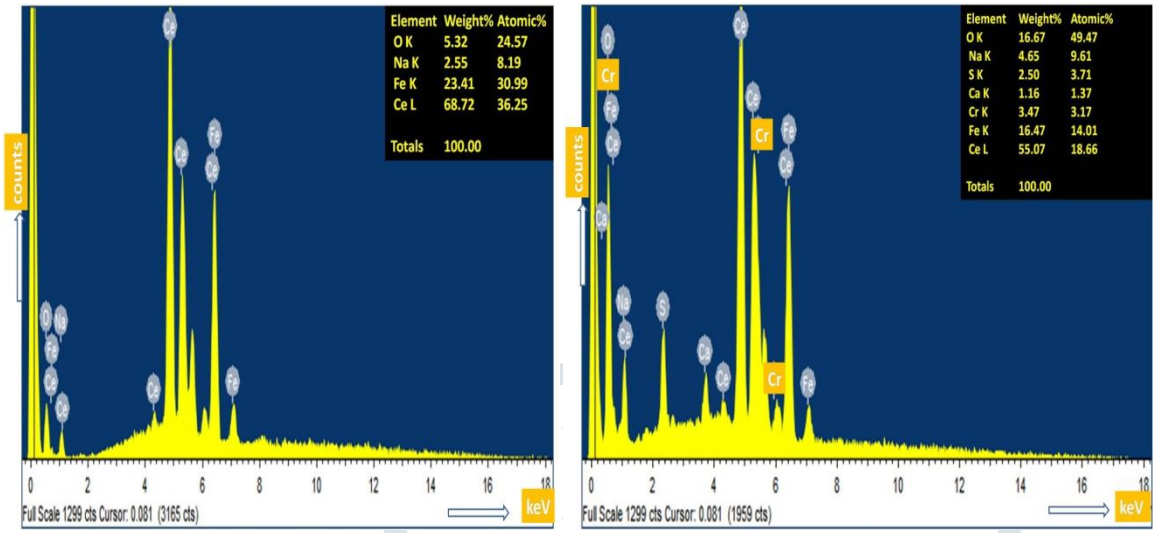

Fig.3 (b) EDAX spectrum CeFeO3 and $CeFe_{1-x}Cr_xO_3$ (x=0, 0.2)

3.4 VSM analysis

The magnetic field dependence of specific magnetization (M-H curve) obtained from VSM measurement for $CeFeO_3$ and $CeFe_{1-x}Cr_xO_3$ nanoparticle designed at room temperature(RT) varying the applied magnetic field in the range of ±15 kOe fig (4). From small hysteresis loop behaviour the sample exhibits week ferromagnetic nature. The magnetic parameter are reported in table1.It can be seen that magnetization, coercivity, Retentivity are decrease from pure and depend (x=0-0.2). The CeFeO3 is antiferromagnetic behaviour due to the super exchange interaction between these neighbouring Fe^{3+} irons of Fe^{3+} - o^{2-} - Fe^{3+}. This behaviour has been observed in the nanoparticle $CeFeO_3$ samples with in $BiFeO_3$ and $YfeO_3$. These loops are not saturated. This indicates that Fe^{3+} spins are not absolutely anti-parallel, but in reality they may be canted. It also indicates that an increase in the Cr content is accompanied by the decrease in the residual magnetization and coercive field. As mentioned before, the ferromagnetism behaviour in our $CeFeO_3$ samples is due to spin canting of Fe^{3+} as the source of the magnetic moments. The magnetic properties of the rare earth orthoferrites are originated from the super exchange interaction between Fe^{3+} - Fe^{3+}, R^{3+} - R^{3+} and R^{3+} - Fe^{3+} via O^{2-} ions.

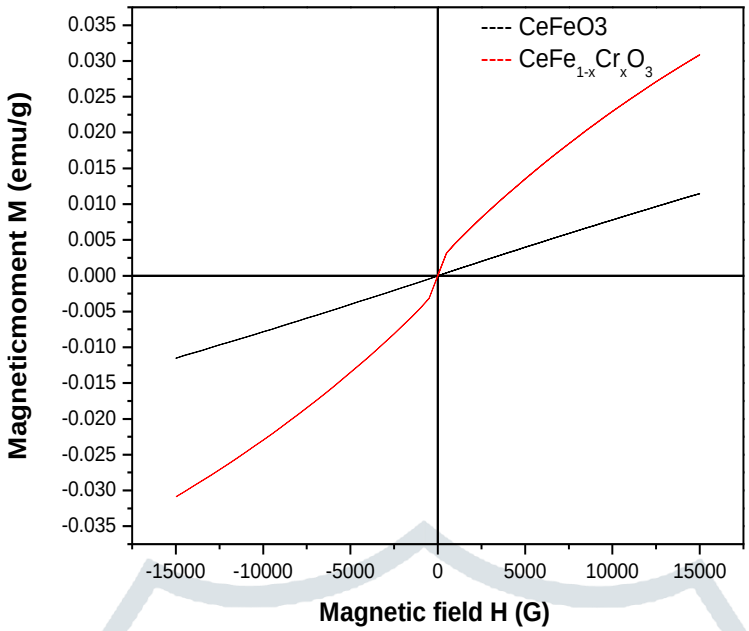

Fig.4 VSM analysis of $CeFe_{1-x}Cr_xO_3$ (x = 0, 0.2)

Table:1

X	0	0.2
CoercivityH$_c$(G)	13.215	13.981
Magnetization M$_s$(emu)	30.885×10^{-3}	11.50×10^{-3}
RetentivityM$_r$ (emu)	85.01×10^{-6}	11.736×10^{-6}
Squareness (M$_r$/M$_s$)	0.00275	0.00102

3.4 CONCLUSION

Nanoparticles of $CeFe_{1-x}Cr_xO3$ (x = 0, 0.2) have been synthesized by Co-precipitation method. The average crystallite size (Dc) is varying between 9nm-24.6nm. The morphology is analysed using scanning electron microscope. The weak ferromagnetic behaviour is observed from hysteresis loop behaviour. Coercivity (Hc), Magnetization and Retentivity are eventually decreasing with 'x' value. At x = 0.2 the maximum value of magnetization shows a potential visible – light – driven photocatalyst in the sunlight-induced photocatalytic degradation of wastewater.

Acknowledgment:

We gratefully acknowledge support from Arignar Govt Arts College- Cheyyar, Tamil Nadu, India. We also express our thanks to IIT Chennai for recording VSM analysis of the samples.

REFERENCES

[1] C.B. Samantaray, H. Sim, H. Hwang, Microelectron. J. 36 (8) (2005) 725.

[2] C.B. Samantaray, H. Sim, H. Hwang, Phys. B 351 (1–2) (2004) 158.

[3] J.G. Bednorz, K.A. Muller, Phys. Rev. Lett. 52 (25) (1984) 2289.

[4] Y. Tokura (Ed.), Advances in Condensed Matter Science, 2, Gordon and Breach, The Netherlands, 2000.

[5] A.J. Millis, B.I. Shraiman, R. Mueller, Phys. Rev. Lett. 77 (1996) 175.

[6] P. Baettig, C.F. Schelle, R. LeSar, U.V. Waghmare, N.A. Spaldin, Chem. Mater. 17 (6) (2005) 1376.

[7] H. Wang, B. Wang, Q. Li, Z. Zhu, R. Wang, C.H. Woo, Phys. Rev. B 75 (2007) 245209.

[8] H.P.R. Frederikse, W.R. Thurber, W.R. Hosler, Phys. Rev. 134 (2A) (1964) A442.

[9].M.B. Bellakki, B. Kelly, V. Manivannan, Synthesis and characterization and property studies of (La, Ag) FeO3 perovskite materials, J. Alloys Compd. 489 (2010) 64–71.

[10] S.A. Mir, M. Ikram, K. Asokan, Structural, optical and dielectric properties of Ni substituted NdFeO3, Optik 125 (2014) 6903e6908.

[11] T.S. Zhang, J. Ma, L.B. Kong, S.H. Chan, J.A. Kilner, Aging behavior and ionic conductivity of ceria-based ceramics: a comparative study, Solid State Ion. 170 (2004) 209e217.

[12] A. Wu, H. Shen, J. Xu, Z. Wang, L. Jiang, L. Luo, S. Yuan, S. Cao, H. Zhang, Crystal growth and magnetic property of YFeO3 crystal, Bull. Mater. Sci. 35 (2012) 259e263.

[13] J. Ameta, A. Kumar, R. Ameta, V.K. Sharma, S.C. Ameta, Synthesis and characterization of CeFeO3 photocatalyst used in photocatalytic bleaching of gentian violet, J. Iran. Chem. Soc. 6 (2009) 293e299.

[14] A. Abbad, W. Benstaali, H.A. Bentounes, S. Bentata, Y. Benmalem, Search for half-

[15] Kudo A, Miseki Y. Heterogeneous photocatalyst materials for water splitting. Chem Soc Rev 2009;38:253e78. http://dx.doi.org/10.1039/b800489g.

[16] Liao C-H, Huang C-W, Wu JCS. Hydrogen production from semiconductor-based photocatalysis via water splitting.Catalysts 2012;2:490e516. http://dx.doi.org/10.3390/catal2040490.

[17] Salgado SYA, Zamora RMR, Zanella R, Peral J, Malato S,Maldonado MI. Photocatalytic hydrogen production in a solar pilot plant using a Au/TiO2 photo catalyst. Int J Hydrogen Energy 2016;41:11933e40. http://dx.doi.org/10.1016/j.ijhydene.2016.05.039.

[18] Sharma D, Verma A, Satsangi VR, Shrivastav R, Dass S. Nanostructured SrTiO3 thin films sensitized by Cu2O for photoelectrochemical hydrogen generation. Int J Hydrogen Energy 2014;39:4189e97. http://dx.doi.org/10.1016/j.ijhyd ene.2013.12.201.

[19] Kudo A, Kato H. Effect of lanthanide-doping into NaTaO3 photocatalysts for efficient water splitting. Chem Phys Lett 2000;331:373e7. http://dx.doi.org/10.1016/S0009-2614(00)01220-3.

[20] J. Ameta, N. Gupta, R. Ameta, *et al.*, Photocatalytic bleaching of alizarin red over CeFeO3 particulate system. *Int. J. Chem. Sci.* **7**(4), 2703–2713 (2009).

[21] R. Lin, and Y. Liang, Preparation and photocatalytic properties of nanosized CeFeO3. *Inorg.Chem. Indus.* **43**(9), 20–22 (2011).

[22] J. Ameta, A. Kumar, R. Ameta, *et al.*, Synthesis and characterization of CeFeO3 photocatalyst used in photocatalytic bleaching of gentian violet. *J. Iran. Chem. Soc.* **6**(2), 293–299 (2009).

[23] Y.S. Didosyan, H. Hauser, G.A. Reider, W. Toriser, J. Appl. Phys. 95 (2004) 7339.

[24] Mahmoud, Mohamed H., et al. "Synthesis of highly ordered 30nm NiFe 2 O 4 particles by the microwave-combustion method." Journal of Magnetism and Magnetic Materials 369 (2014): 55-61.

[25] Tugova, E. A., et al. "Phase diagram of the LaFeO3-LaSrFeO4 system." Glass Physics and Chemistry 32 (2006): 674-676.

[26] Petrović, S., et al. "LaMO3 (M= Mg, Ti, Fe) perovskite type oxides: preparation, characterization and catalytic properties in methane deep oxidation." Applied Catalysis B: Environmental 79 (2008): 186-198.